Recycling experiments for sludge monitoring in waste water treatment*

Sandro Maquiné de Souza
Heudiasyc, UMR CNRS 6599
B.P. 20529
Université de Technologie de Compiègne
60205 Compiègne Cedex, France
maquine@hds.utc.fr

Thierry Denoeux
tdenoeux@hds.utc.fr

Yves Grandvalet
grandval@hds.utc.fr

Abstract - *Belt filter presses are widely used to remove water from residual sludge generated in wastewater treatment plants. The texture (fine or coarse) of the conditioned sludge is a relevant piece of information used by operators to control the dewatering equipment. A software sensor, which takes digital images as input and outputs a signal that is correlated to sludge dry content, was developed. This signal can be used as an input to an automated control system. To characterize the textures, features were computed by the use of a bank of Gabor filters. A model that ranks images according to their corresponding dry contents was calibrated from a database composed of digital images and dry content analysis results. A control system using this information makes it possible to reduce human intervention which is, till today, essential to assure proper operation of belt filter presses.*

Keywords: Belt filter press, Gabor filters, texture classification, wastewater treatment, software sensor, sludge dewatering, image analysis.

1 Introduction

The implementation of European regulations about waste water treatment [3] leads to a significant increase in the municipal residual sludge production (from 5.5 million tonnes of dry matter in 1992 to nearly 9 million tonnes by the end of 2005 in the late European Community). The improvement in the devices used to achieve the volume reduction of this waste is an important step to reduce the cost of the treatment.

Belt filter presses (Figure 1) have been used in European wastewater treatment plants to dewater sludge since the 1960s. The advantage of this equipment is that it performs a continuous treatment of the sludge, with low-energy consumption [1, 2].

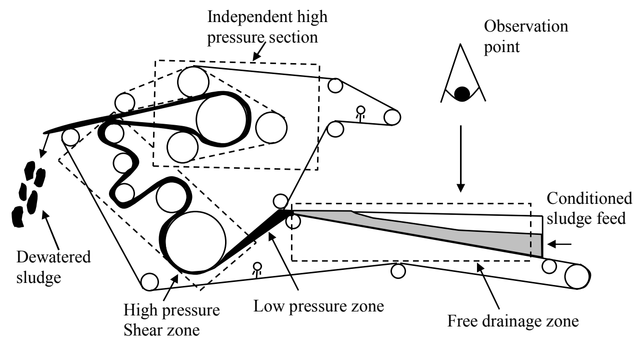

Figure 1. Belt filter press scheme with observation point.

Since these machines can be manually regulated by the observation of the sludge texture, image analysis provides a potentially useful and economic means to automate this process. A set of experiments aiming at studying the feasibility of the video monitoring have been performed. In each experiment, a set of sludge's pictures were taken by a digital camera from the drainage zone during belt press operation, and the dry content of the belt-press-dewatered sludge was measured by sampling the output sludge stream. The water content analysis protocol, which is timely and requires costly human intervention was tested and developed during the data collection process. As a result, only the very last set of experiments provides faithful dryness measurements. This paper proposes to use ranking techniques, which were originally proposed to process preference data [7], in order to take advantage of the entire set of experiments.

An ordinal regression technique [7] was used to compare pairs of images. As a result, a set of images can be ordered in terms of their relative dry content. This information can be used for the design of an automatic control system of the belt filter press.

Sludge dewatering is preceded by a conditioning operation to enhance water removal efficiency. In the conditioning process, chemical coagulants or polymers are added to promote sludge particle aggregation for easier dewatering.

The sludge images are composed of similar textures, but the ones that correspond to low dry contents (less than 14 %) show smoother textures, and the ones that correspond to high dry contents (more than 16 %) show coarser textures [11]. Examples can be seen in Figure 2.

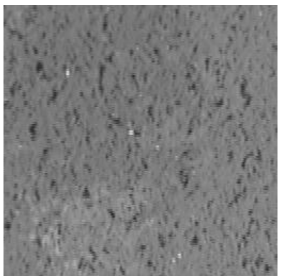

Badly conditioned sludge texture

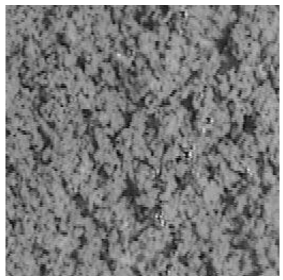

Well conditioned sludge texture

Figure 2. Images gathered from the observation point indicated in Figure 1. Badly conditioned sludge has fine texture and well conditioned sludge has coarse texture

A summary of the belt filter press operation status with regard to dry content in dewatered sludge can be seen in Table 1.

Table 1 – Belt filter press operation status versus dewatered sludge dry content. Source: Waste water treatment plant staff (Mesnil-en-Thelle, France)

Dewatered sludge Dry Content (DC)	*Classification of belt filter press operation*
DC < 14%	Defective
14% < DC < 16%	Acceptable
16% < DC < 18%	Good
DC > 18%	Excellent

This work aims to study the feasibility of a control system based on image analysis for a sludge dewatering machine. To do so, the following steps have been followed:

- Use of a database containing digital images and their corresponding dry content analyses;
- Extraction of useful information from the images: computation of features which are sensible to texture, as Gabor Energy;
- Manual ranking of selected images with respect to their relative dry content;
- Development and calibration of a model that ranks the values of the controlled variable (dry content) from a pair of images acquired at different moments;
- Verify that the model correctly ranks the images from the database (images used to calibrate the model and other images).

The use of a rank model, instead of a model that would directly calculate the dry content, is preferable because the current image database has few reliable values of dewatered sludge dry content (due to the use of inadequate procedures for sludge sampling at first sessions). Also, knowing that coarse textures with a considerable space for interstitial water (holes in texture) correspond to dewatered sludge with high dry content, the images can be manually ranked in terms of their dry content by vision [11].

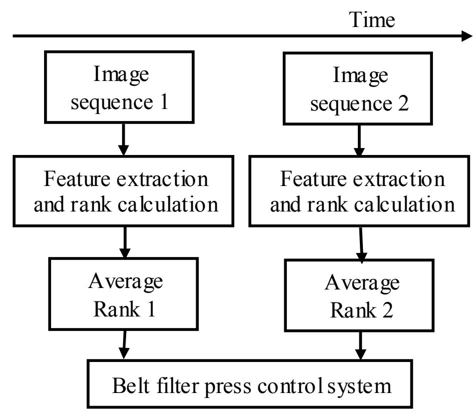

Figure 3. Possible assembly to generate and send input signals to the control system (average ranks 1 and 2). The rank is calculated from the sludge texture and is related to the dewatered sludge dry content (monotonic relation)

2 Methodology

2.1 Image database

Selected images from 4 experimental sessions were manually ranked, according to their texture and corresponding dry contents. Each image is originally 704 pixels wide and 576 pixels high, approximately 20 cm wide and 17 cm high. Table 2 summarizes this database.

Table 2 – Image database used for feature extraction and model calibration. There are 4 experimental sessions and up to 3 ranks per session. Each image sample is part of a group of 5 similar images. Total number of images is 55

Ses-sion	Rank determined by operator → Increasing roughness		
	1	2	3
1	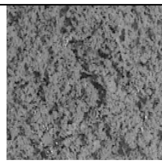 DC = 14.1 %	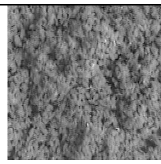 DC = 14.7 %	
2	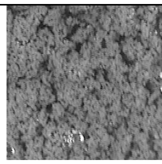 DC = 13.9 %	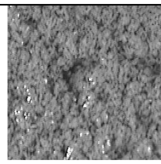 DC = 14.4 %	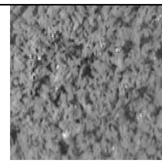 DC = 15.5 %
3	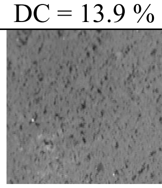 DC = 12.7 %	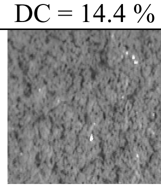 DC = 13.9 %	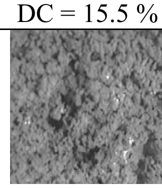 DC = 15.9 %
4	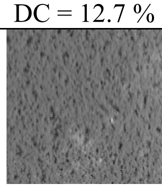 DC = 13.0 %	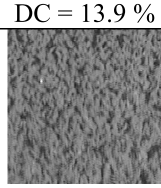 DC = 15.3 %	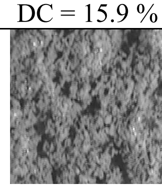 DC = 16.0 %

2.2 Feature Extraction from Images

Co-occurrence matrix and Gabor filter based techniques are among the most efficient approaches to texture analysis [6, 9]. Gabor filter features include Gabor filter response, complex features, Gabor Energy features and Grating Cell operators [5].

In this work, global Gabor-filter-based features were used. Global features are calculated over a whole image. The central portion of every image (512 x 512 pixels) is used for feature extraction.

The image $i(x, y)$, $(x, y) \in \Omega$ (Ω is the set of image points) is convolved with a 2 dimensional Gabor function $g(x, y)$, $(x, y) \in \Omega$ to obtain a Gabor feature image $r(x, y)$. The Gabor function used in the spatial domain is:

$$g(x,y) = \exp\left(-\frac{1}{2}\left(\frac{x'^2}{\sigma_x^2}+\frac{y'^2}{\sigma_y^2}\right)\right)\cos(2\pi f\, x')\,, \qquad (1)$$

where $x' = x\cos\theta + y\sin\theta$, $y' = -x\sin\theta + y\cos\theta$;

f is the frequency of a sinusoidal plane wave, θ is the anti-clockwise rotation of the Gaussian envelope and the sinusoid, and σ_x and σ_y are the space constants of the Gaussian envelope along the x and y axes, respectively.

The Fourier domain representation of (1) is given by

$$G(u,v) = A\left(\exp\left\{-\frac{1}{2}\left(\frac{(u'-f)^2}{\sigma_u^2}+\frac{v'^2}{\sigma_v^2}\right)\right\} + \exp\left\{-\frac{1}{2}\left(\frac{(u'+f)^2}{\sigma_u^2}+\frac{v'^2}{\sigma_v^2}\right)\right\}\right), \qquad (2)$$

where $\sigma_u = 1/(2\pi\sigma_x)$, $\sigma_v = 1/(2\pi\sigma_y)$, $A = 2\pi\sigma_x\sigma_y$, $u' = u\cos\theta + v\sin\theta$, $v' = -u\sin\theta + v\cos\theta$.

The Gabor filter bank used herewith follows the specifications of Jain & Farrokhnia [8]. Frequencies and orientations used were:

$f \in \{\sqrt{2}, 2\sqrt{2}, 4\sqrt{2}, \ldots, 128\sqrt{2}\}$ cycles / image-width,
$\theta \in \{0°, 45°, 90°, 135°\}$.

The feature image R is computed by a convolution in the Fourier domain, an element-wise multiplication:

$$R_{f,\theta}(u,v) = G_{f,\theta}(u,v)\,.\,I(u,v), \qquad (3)$$

where I(u,v) is the image represented in the Fourier domain.

The total energy of the 2D signal (feature image) is used as a feature:

$$E_{f,\theta} = \sum_{u,v}\left|R_{fo,\theta}(u,v)\right|^2 . \qquad (4)$$

No relevant information is expected from different orientations (texture properties are supposed to be invariant to rotation).

The energy from every orientation is added to give only one feature per frequency:

$$E_f = \sum_j E_{f,\theta_j} . \qquad (5)$$

The total number of features per image is 8.

2.3 Model for ordinal regression

The images were acquired during 4 distinct experience sessions, but reliable water content analyses are only available during the last session. The images gathered in the first experiments do, however, convey partial information regarding the water content: while the analyses pertaining to two sets of experiments cannot be compared, some of the pairs of images recorded during one session can be ranked according to their relative water content. This type of information cannot be used for the sludge dryness prediction itself, but one can use it to extract relevant image features.

The ranking technique based on the margin concept of support vector machines (SVMs) [12] proposed by Herbrich *et al*. [7] was used to extract features from the pairwise image comparisons.

Note that another approach could have been proposed, where classes could be defined based on dry matter content values (e.g. class labels = "low dry content", "medium dry content", "high dry content"). Then an ordinal regression technique [10] could be applied. However, the precision of dry content value being unknown, we prefer to deliver a less accurate but more confident information to the statistical inference scheme. Also, in order to work with categories, it is necessary to compare data from several experimental sessions. With the approach used in this work, data from a sole session are compared, independently from the data from other sessions.

Let $\underline{x}$ be the feature vector of an image:

$$\underline{x} = [x_1, x_2, ..., x_d]^{\mathrm{T}} \tag{5}$$

where d is the total number of features.

The model output $y(\underline{x})$ is a real scalar value, the rank of the image:

$$\begin{aligned} y(\underline{x}) &= \underline{w}^T \underline{x} \\ \underline{w} &= [w_1, w_2, ..., w_d]^T \end{aligned} \tag{6}$$

where $\underline{w}$ is the parameter vector of the model.

For every pair of images, ordered with respect to their corresponding dry contents:

$\mathrm{Image_i} \succ \mathrm{Image_j}\,; i, j \in \{1, 2, ..., n\}$, where n = total number of images, the model should ensure that:

$$y(\underline{x}_i) > y(\underline{x}_j) \Rightarrow \underline{w}^T \underline{x}_i > \underline{w}^T \underline{x}_j\,, \tag{7}$$

and an arbitrary separation between ranks should be chosen. To simplify the calculations, we choose this value to be 1:

$$\underline{w}^T \underline{x}_i \geq \underline{w}^T \underline{x}_j + 1\,. \tag{8}$$

Let $\underline{\underline{R}}$ be the logical matrix of ordered pairs of images (lower triangular matrix):

$$\underline{\underline{R}} = \left[\begin{array}{c|cccc} & j=1 & j=2 & ... & j=n \\ \hline i=1 & 0 & 0 & ... & 0 \\ i=2 & R_{2;1} & 0 & ... & 0 \\ ... & ... & ... & ... & \\ i=n & R_{n;1} & R_{n;2} & ... & 0 \end{array}\right] \tag{9}$$

$$R_{i;j} = \begin{cases} 1, \text{if } \mathrm{Image_i} \succ \mathrm{Image_j} \\ 0, \text{otherwise} \end{cases}$$

Let $\underline{I}$ and $\underline{J}$ be the vectors of indices of $\underline{\underline{R}}$ where $R_{i;j} = 1$, $i \in \underline{I}$ and $j \in \underline{J}$:

$\underline{I} = [i_1, i_2, \ldots, i_m]$, $\underline{J} = [j_1, j_2, \ldots, j_m]$

where m = total number of ordered pairs, $m = \sum_{i;j} R_{i;j}$

The optimization problem can be written as follows:

$$\begin{aligned} &\min_{\underline{w}} \frac{1}{2}\|\underline{w}\|^2, \text{subject to } \underline{w}^T(\underline{x}_{I_k} - \underline{x}_{J_k}) \geq 1 \\ &\forall k \in \{1,2,...,m\} \end{aligned} \tag{10}$$

In order to take model imperfections into account (badly determined ranks or incompatible orderings from different experimental sessions), a slack variable is introduced for every constraint equation. These slack variables should be as small as possible, and non-negative. The optimization problem is then rewritten as follows:

$$\begin{aligned} &\min_{\underline{w},\underline{\xi}} \left\{ \frac{1}{2}\|\underline{w}\|^2 + c\sum_{k=1}^{m} \xi_k \right\}, \text{subject to } \begin{cases} \underline{w}^T(\underline{x}_{I_k} - \underline{x}_{J_k}) \geq 1 - \xi_k \\ \xi_k \geq 0 \end{cases} \\ &\forall k \in \{1, 2, ..., m\} \end{aligned} \tag{11}$$

In equation (11), in addition to the new parameters to estimate (slack variables, vector $\underline{\xi}$), the value of the hyperparameter c should also be chosen. This can be done by cross-validation.

The problem is solved by a quadratic programming algorithm similar to the one described in [4]: the routine *quadprog* from Matlab® optimization toolbox.

3 Results

3.1 Determination of the hyperparameter *c*

To determine the hyperparameter c, a cross-validation was performed. One optimization is done per experimental session. In each one of these optimizations, data from 3 experimental sessions are used. For the excluded session, we compute a vector of slack variables, $\underline{\xi}^{(E)}$, by (12):

$$\underline{\xi}^{(E)} = \underline{1} - \begin{bmatrix} \underline{w}^T(\underline{x}_{i_1} - \underline{x}_{j_1}) \\ \dots \\ \underline{w}^T(\underline{x}_{i_e} - \underline{x}_{j_e}) \end{bmatrix} \qquad (12)$$

where e is the number of ordered pairs for the excluded session, $e < m$. The sum of the positive values of $\underline{\xi}^{(E)}$ is used to evaluate the choice of c. See figure 4.

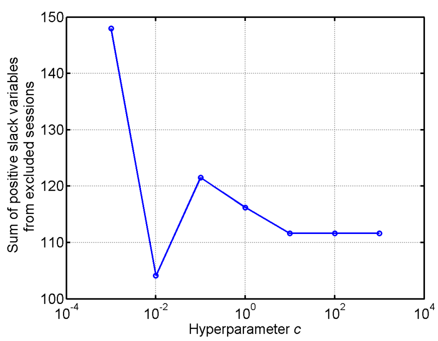

Figure 4. Choice of hyperparameter c. $c = 10^{-2}$ corresponds to the lowest error

In Figure 5, manually determined ranks are plotted versus model output. With the exception of the session 2 (Figure 6), where images were not easily distinguishable by their texture (Table 2), all ranks have a good separation with a difference of nearly 1, as shown in equation (10). Single symbols (◀ , ▼ or ▶) represent single images.

Reliable dry content analyses were performed during experimental sessions 3 and 4. In Figure 6, model output is plotted versus dry content values. A monotonic relation between these variables can be noticed. Values from sessions 1 and 2, compared to values from sessions 3 and 4, do not present a perfect monotonic relation, which justifies a two-step model calibration (by rankings and then by regression). The results for session 2 indicate that data from this session should perhaps not be used to calibrate the model.

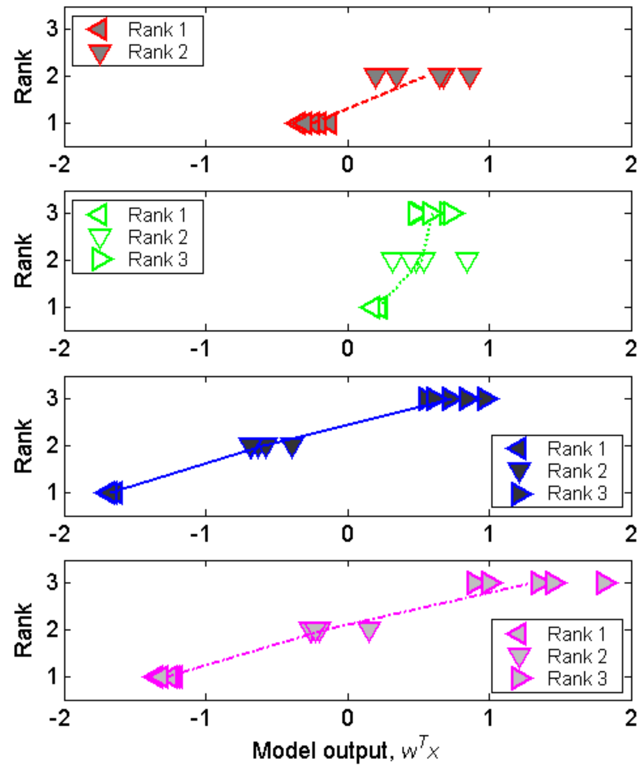

Figure 5. Model response versus manually determined ranks for all experimental sessions

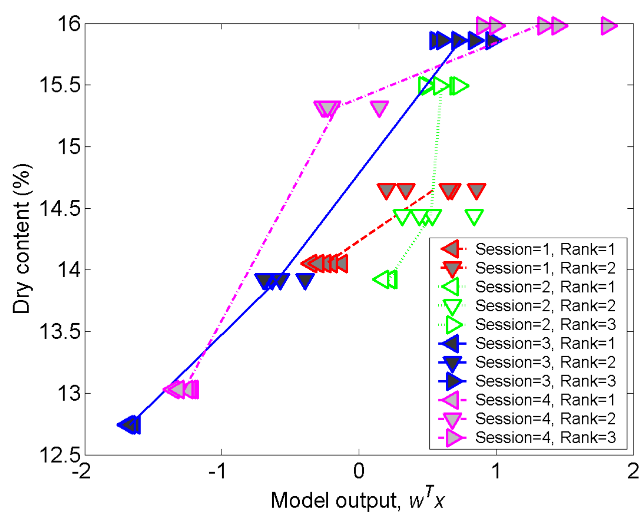

Figure 6. Model responses versus available dry content values for all experimental sessions. Indicated ranks are manually determined ranks.

Figure 7 shows historical data from session 4 and model response for all images from this session. Very low values correspond to abnormal operation. Excluding these situations, the model output has the same trend as the dry content values.

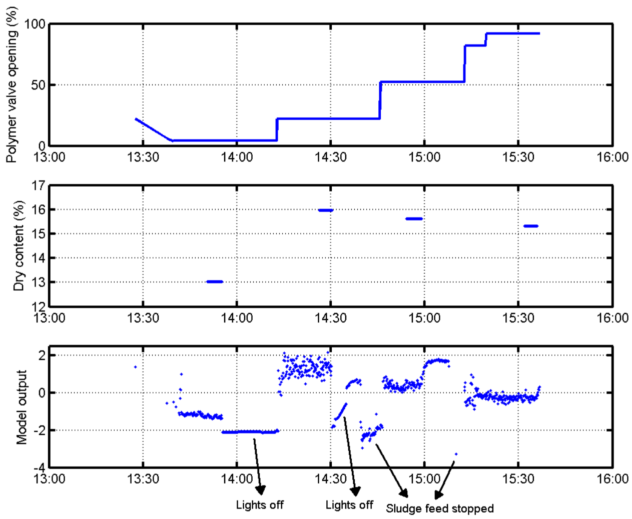

Figure 7. Experimental session number 4. Historical data (polymer valve opening, dry content) and model response

4 Conclusions and Outlook

Belt filter presses are widely used to remove water from the residual sludge generated in wastewater treatment plants. Their proper operation requires considerable human intervention for maintenance and control.

In this work, a new software sensor has been proposed, which outputs a signal correlated with the dewatered sludge dry content. The input signals are images gathered from a particular point of the belt filter press.

A database composed of digital images and dry content values was used to calibrate a model, whose output, the rank, is an indirect measure of the dewatered sludge dry content. To calibrate the model, no dry content values were directly used; instead, some pairs of images were manually ranked in terms of their corresponding dry content values. These images were ranked with regard to their texture (fine or coarse). Conditioned sludge texture constitutes key information used by operators to control the belt filter press.

A number of features were calculated from the digital images. These features are the total energy of the 2D signal computed from the convolution of the images with 8 different Gabor functions (8 different central frequencies). The feature vector is the input to the model.

The results show a good correlation between the model output and the available dry content values. The ranks calculated by the model can be used as an input to control systems.

In a future work, a model that outputs dewatered sludge dry content values can be developed. But before this can be done, it is necessary to build a database with more reliable dry content analysis.

References

[1] Dembitz, A.E. (1978). Belt filter presses: a new solution to dewatering? *Water Environment and Technology*, 15, 36-42.

[2] Deutsh N.D. (1987). Options in belt filter press. *Water Engineering and Management*, 134, issue 9, 34-37.

[3] European Union (1991). Council Directive of 21 May 1991 concerning urban waste water treatment (91/271/EEC). *Official Journal of the European Union*, L 135, 30.05.1991, p. 40. Luxembourg.

[4] Gill, P. E. and W. Murray, and M.H. Wright, Practical Optimization, Academic Press, London, UK, 1981.

[5] Grigorescu, S.E., Petkov, N., Kruizinga, P. (2002). Comparison of Texture Features Based on Gabor Filters. *IEEE Transactions on Image Processing*, 11, 1160-1167.

[6] Haralick, R., Shanmugam K. and Dinstein, I. (1973). Texture features for image classification. *IEEE Trans. Syst. Man Cybernet*. 3, pp. 610–621.

[7] Herbrich, R., Graepel, T. and Obermayer, K. (2000). Large Margin Rank Boundaries for Ordinal Regression. *In* Advances in Large Margin Classifiers, pages 115-132.

[8] Jain, A.K. and Farrokhnia, F. (1991). Unsupervised texture segmentation using Gabor filters. *Pattern Recognition*, 24, 1167-1186.

[9] Kruizinga, P., Petkov, N. (1999). Nonlinear Operator for Oriented Texture. *IEEE Transactions on Image Processing*, 8, 1395-1407.

[10] McCullagh, P. and Nelder, J.A. (1983). Generalized Linear Models. Chapman and Hall, London.

[11] OTV (1997). Traiter et valoriser les boues (in French), pp. 217-225, Infinités Communication, Rennemoulin, France.

[12] Vapnik, V. N. (1995). The nature of statistical learning theory. Springer, New York (USA). ISBN 0-387-94559-8.